Indian Geotechnical Journal, 30 (2), 2000

Lateral Displacement Interaction between Soil and Reinforcement Strip

N. Kumar Pitchumani* and M.R. Madhav†

Introduction

Reinforced foundation beds show a good improvement in the bearing capacity and in reducing foundation settlements. In this pursuit, soil reinforced with strips, fabrics, sheets, grids and cells are becoming very common. Research is being carried out to study the effect of reinforcing elements below foundations in increasing the bearing capacity of foundations, all around the globe. One of the pioneering studies was carried out by Binquet and Lee (1975). Finite Element studies (Love et al., 1988, Andrawes and McGown, 1982) have helped predict the increase in bearing capacity of reinforced foundation beds. A number of model and field studies (Fragaszy and Lawton 1984, Miura et al. 1985; Huang and Tatsuoka, 1988; Jones and Dawson, 1990) establish the improvement in foundation response and bearing capacity due to reinforcement of soil. Few analytical (Giroud and Noiray, 1981; Houlsby and Jewell, 1990) studies are also available. Models using Pasternak shear layers and Winkler type subgrade have been proposed (Madhav and Ghosh, 1988) for settlement analysis of reinforced soils. It is seen that there are a very few studies to predict the settlement behaviour of reinforced foundation beds. Settlements play a major role in designing of pavements. Hence it is essential that the reductions in surface settlements due to embedded reinforcements be estimated. The present study proposes a method to predict the reduction in surface settlements due to strip form of reinforcements placed beneath a rectangular loaded area. The elastic continuum approach is adopted to solve the problem. The shear interaction of reinforcing strips is considered.

---

* Assistant Professor, Department of Civil Engineering, Indian Institute of Technology, Chennai – 600036, India.

† Professor, Department of Civil Engineering, Indian Institute of Technology, KANPUR – 208016, India.

Problem Definition

A strip of size, $2L_r \times 2B_r$, is placed at a depth, U_0, centrally below a rectangular area of size, $2L_f \times 2B_f$, transmitting a uniform load of intensity q (Fig. 1). The width of the strip, $2B_r$, is relatively small ($0.1B_f$) and thickness, t_r, negligible. The surface load causes vertical and lateral displacements of points in the soil. The interaction of the soil and strip for vertical displacements has been explained elsewhere (Pitchumani and Madhav, 1994). The lateral displacements are restrained by strip reinforcement and as a result shear stresses are mobilised at the interface (Fig. 2). An extensible strip will experience elongation while an inextensible one will not. The magnitude of these shear stresses will depend on the axial stiffness of the strip. These stresses are symmetric about the vertical axis due to symmetry of the loading and geometry.

Since the outward lateral movement of the soil at the strip-soil interface is prevented by the mobilisation of shear stresses at the interface, these stresses are directed inward, towards the centre of the strip. These stresses in turn introduce tension in the strip (Fig. 3). The net result of these mobilised stresses is to push the soil on the surface upward near the centre of the loaded area. Consequently, there is a reduction in settlements of points along the surface. Thus the reinforcing strip helps in reducing foundation settlements.

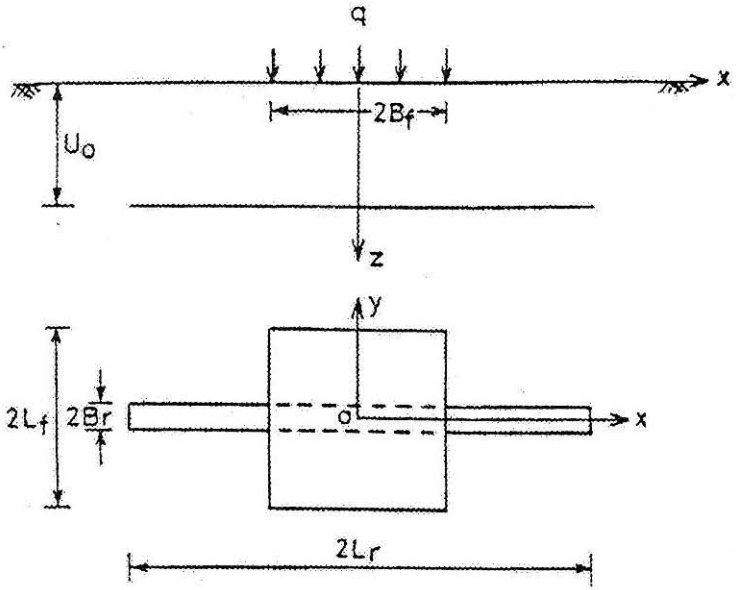

FIGURE 1 : Definition Sketch

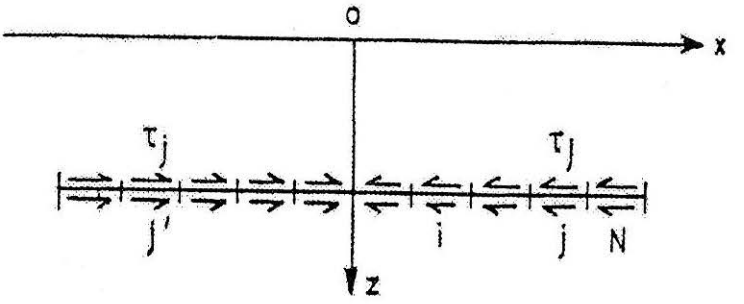

FIGURE 2 : Shear Stresses at the Interface

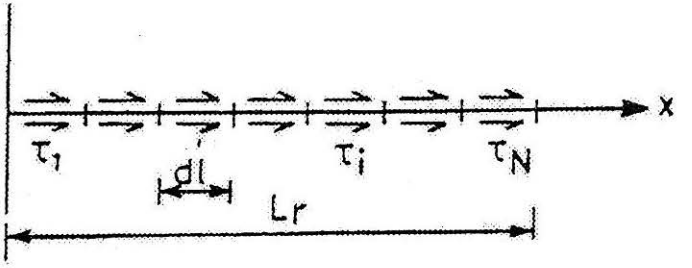

FIGURE 3 : Stresses on the Strip

Formulation

The elastic continuum approach is resorted to study the soil-reinforcement interaction. The soil is assumed to be homogeneous, isotropic, linearly elastic and semi-infinite in nature. Due to symmetry only half the strip is considered which is divided into N elements and over each element, the shear stress is assumed to be uniform.

The horizontal displacement, ρ_{xi}^{f}, of node i, along the reinforcement, due to a uniform surface load, q, is obtained by integrating the Boussinesq's equation for lateral displacements due to a point load on the surface, over the loaded area as

$$\rho_{xi}^{f} = \int_{-B_f}^{B_f}\int_{-L_f}^{L_f} \frac{q(1+\nu_s)}{2\pi E_s R}\left(\frac{rU_0}{R^2} - \frac{(1-2\nu_s)r}{(R+U_0)}\right)\cos\alpha \cdot dA \qquad (1)$$

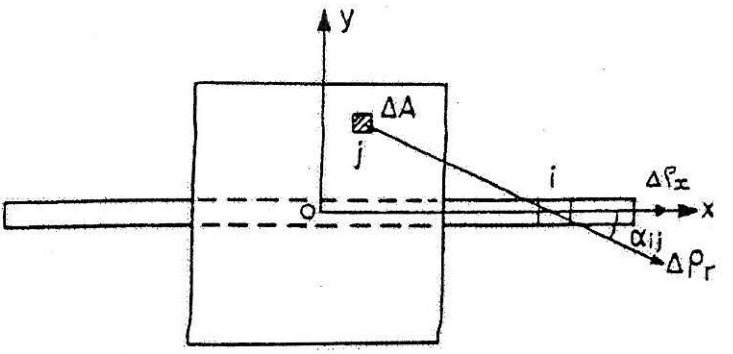

FIGURE 4 : Radial and Horizontal Displacements along Strip due to Surface Load

where $R = \sqrt{r^2 + U_0^2}$

r = radial distance of node i, from the elemental area dA on the surface (Fig. 4)

U_0 = depth of node i, from the elemental area dA on the surface (Fig. 4)

E_s = modulus of deformation of the soil treated as a continuum.

n_s = Poisson's ratio of the soil treated as a continuum.

The integration is performed numerically. For this purpose, the width of the loaded area is divided into 'n_b' elements and the length into 'n_l' elements. The vertical displacement of the i^{th} node along the reinforcement is then expressed as

$$\rho_{xi}^{f} = \sum_{i_r=1}^{n_b}\sum_{j_r=1}^{n_l} \frac{q(1+\nu_s)}{2\pi E_s R}\left(\frac{rU_0}{R^2} - \frac{(1-2\nu_s)r}{(R+U_0)}\right)\cos\alpha \cdot dA \qquad (2)$$

where $r = \sqrt{x^2 + y^2}$,

x and y = cartesian co-ordinates of node i,

U_0 = depth of placement of the strip and

dA = elemental area.

Non-dimensionalising all length parameters with half-width B_f, of the loaded area, Eqn. 2 is expressed as

$$\rho_{xi}^{f} = \frac{B_f}{E_s} I_i^f q \tag{3}$$

where I_i^f is a dimensionless influence coefficient that depends on the aspect ratio, L_f/B_f, of the loaded area, depth, U_0/B_f, of the strip, Poisson's ratio of the soil and the location of node i.

The vector of horizontal displacements $\{\rho_x^f\}$ of all the nodes along the half-length of the strip is obtained by evaluating Eqn. 3 for all N nodes as

$$\{\rho_x^f\} = \frac{B_f}{E_s}\{I^f\} q \tag{4}$$

where the vectors $\{\rho_x^f\}$ and $\{I^f\}$ are of size N.

The horizontal displacement, ρ_{zij}^{rl} at node i, along the strip due to shear stress, τ_j, acting on element j along the strip is computed using Mindlin's equation for displacements due to a vertical force acting beneath the surface of a semi-infinite medium as

$$\{\rho_{xij}^{rl}\} = \frac{\tau_j(1+\nu_s)\Delta A}{8\pi E_s(1-\nu_s)}(F) \tag{5}$$

where

$$F = \frac{(3-4\nu_s)}{R_1} + \frac{1}{R_2} + \frac{x^2}{R_1^3} + \frac{(3-4\nu_s)x^2}{R_2^3} + \frac{2cz}{R_2^3}\left(1-\frac{3x^2}{R_2^2}\right) + \frac{4(1-\nu_s)(1-2\nu_s)}{(R_2+z+c)}\left(1-\frac{x^2}{R_2^2(R_2+z+c)}\right)$$

$$R_1 = \sqrt{x^2+y^2+(z-c)^2}$$

$$R_2 = \sqrt{x^2+y^2+(z+c)^2}$$

x and y = horizontal distances of node i with respect to the elemental area, ΔA, of the j^{th} element and

$c = U_0 = z$.

Equation 5 is evaluated numerically as

$$\rho_{xij}^{rl} = \frac{B_f}{E_s} I_{ij}^{rl} \tau_j \tag{6}$$

where I_{ij}^{rl} is a dimensionless influence coefficient that depends on the parameters and ν_s and locations of elements i and j. For every element j, there exists its image j', shear stress on which is the same as that acting on element j. The influence of the stress acting on element j' on the horizontal displacement of node i is

$$\rho_{xij}^{r2} = \frac{B_f}{E_s} I_{ij}^{r2} \tau_j \tag{7}$$

where I_{ij}^{r2} is a displacement influence coefficient for the influence of the stress on element j', on the horizontal displacement of node i.

The shear stress, τ_j, on elements j and j' act in opposite directions and hence the displacements due to shear stress on each of these elements will be in opposite directions. Combining Eqns. 6 and 7, the net horizontal displacement of node i due to shear stresses on all the N elements is

$$\rho_{xi}^{r} = \sum_{j=1}^{N} \frac{B_f}{E_s} \left(I_{ij}^{rl} - I_{ij}^{r2} \right) \tau_j \tag{8}$$

The vector of horizontal displacements, $\{\rho_x^r\}$, of all N nodes is expressed as

$$\{\rho_s^r\} = \frac{B_f}{E_s} [I^r] \{\tau\} \tag{9}$$

where vectors $\{\rho_x^r\}$ and $\{\tau\}$ are of size N and $[I^r]$ is a square matrix of size N and whose elements are $I_{ij}^r = I_{ij}^{rl} - I_{ij}^{r2}$ and $I_{ij}^r = I_{ji}^r$

The net soil displacement vector, $\{\rho_z^s\}$ is obtained from the difference of Eqn. 4 and Eqn. 9 expressed as

$$\{\rho_x^s\} = \{\rho_x^f\} - \{\rho_x^r\} \tag{10}$$

Inextensible Strip

If the strip is inextensible, the net soil displacements equal to 0, i.e.

$$\{\rho_x^f\} - \{\rho_x^r\} = \{0\} \tag{11}$$

Combining Eqns. 4, 9 and 11, one obtains

$$[I^r]\left\{\frac{\tau}{q}\right\} = \{I^f\} \tag{12}$$

Equation 12 gives N equations for the shear stresses, , which are solved by the Gauss elimination technique.

These shear stresses are developed at the interface of the soil and strip. The thickness of the strip being negligibly small, it can be assumed that the stresses above and below the strip are equal to half the calculated values. The stresses mobilised in the soil in turn develop tension in the reinforcing strip. The total tension to the left of the i^{th} element is expressed as under.

$$T_i = \sum_{j=i}^{N} \tau_j dl 2 B_r \tag{13}$$

Extensible Strip

For an extensible strip, the net soil displacements equal the strip elongations, and are expressed as

$$\{\rho_z^f\} - \{\rho_z^r\} = \{\rho_e\} \tag{14}$$

The elongations are introduced because of the tension in the strip. The elemental elongation, $\Delta\rho_{ek}$ of the k^{th} element is

$$\Delta\rho_{ek} = \left(T_k + \frac{\Delta T_k}{2}\right)\frac{dl}{A_r E_r} \tag{15}$$

where $A_r = 2B_r t_r$ is the cross sectional area of the strip, and E_r is the modulus of elasticity of the strip. Substituting Eqn. 13 in Eqn. 15 one obtains

$$\Delta\rho_{ek} = \left(\frac{\tau_k}{2} + \sum_{i=k+1}^{N}\tau_i\right)\frac{dl^2}{t_r E_r} \tag{16}$$

The total elongation of node k is equal to the sum of all elemental elongations from node 1 to k, and is written as

$$\rho_{ek} = \sum_{j=1}^{k}\Delta\rho_j \tag{17}$$

Combining Eqns. 16 and 17 one obtains the vector of elongations of all the N nodes as

$$\{\rho_e\} = \frac{dl^2}{t_r E_r}[I_e]\{\tau\} \tag{18}$$

where $[I_e]$ is a square elongation coefficient matrix of size N, and is given by

$$[I_e] = \begin{bmatrix} 0.5 & 1.0 & .. & 1.0 \\ 0.5 & 1.5 & 2.0 & 2.0 \\ 0.5 & 1.5 & 2.5 & 3.0 \\ 0.5 & 1.5 & 2.5 & N-0.5 \end{bmatrix}$$

Non-dimensionalising the length parameters with B_f Eqn. 18 is rewritten as

$$\{\rho_e\} = \frac{B_f(dl/B_f)^2}{(t_r/B_f)E_s}[I_e]\{\tau\} \tag{19}$$

Substituting for $\{\rho_e\}$ in Eqn. 14 one obtains

$$\left[[I^r] + \frac{m}{K_\tau}[I_e]\right]\left\{\frac{\tau}{q}\right\} = \{I^f\} \tag{20}$$

where $m = (dl/B_r)^2$ and

$$K_r = \frac{E_r t_r}{E_s B_f}$$

(It is a dimensionless elongation factor which takes into account the axial stiffness of the strip and the modulus of the soil.)

Equation 20 gives N equations for the normalised shear stresses $\{\tau/q\}$, which are solved using the Gauss elimination technique. The tension in the strip is evaluated from Eqn. 13.

Settlement Reduction

The surface heave profile or the settlement reduction, due to the shear stresses mobilised at the soil-strip interface is arrived at by integrating Mindlin's equation for vertical displacement due to a horizontal force within an elastic continuum. The vertical displacement ρ_{zk} of any point k due to a horizontal force, $\tau_j \Delta A$, beneath the surface of a continuum, is

$$\rho_{zk} = \frac{(1+\nu_s)x}{8\pi E_s(1-\nu_s)}(D)\tau_j \Delta A \qquad (21)$$

where

$$D = \frac{(z-c)}{R_1^3} + \frac{(3-4\nu_s)(z-c)}{R_2^3} + \frac{6cz(z+c)}{R_2^5} + \frac{4(1-\nu_s)(1-2\nu_s)}{R_2(R_2+z+c)}$$

and the other terms are as defined in Eqn. 5.

To obtain the vertical displacement of any point k, along the x-axis on the surface due to the shear stress, τ_j, on element j, the following substitutions are made: $z = 0$, $c = U_0$, $R = \sqrt{x^2 + U_0^2}$ and $G_s = E_s/2(1+\nu_s)$. Eqn. 21 then reduces to

$$\rho_{0kj} = \frac{1}{4\pi G_s} \int_{\Delta A} x_{kj} \left[\frac{(1-2\nu_s)}{R(R+U_0)} - \frac{U_0}{R^3} \right] \tau_j \Delta A \qquad (22)$$

where x_{kj} is the distance along the x axis between point k and node j

Equation 22 is rewritten as

$$\rho_{0kj}^{r1} = \frac{B_f}{G_s} I_{0kj}^{r1} \tau_j \tag{23}$$

Displacement at point k due to the shear stress τ_j, on the image element j', on the left half of the strip is

$$\rho_{0kj}^{r2} = \frac{B_f}{G_s} I_{0kj}^{r2} \tau_j \tag{24}$$

Combining Eqns. 23 and 24, for the influence due to stresses on all elements, the vector of vertical surface displacements, $\{\rho_0^r\}$ is

$$\{\rho_0^r\} = \frac{B_f}{G_s}[I_0^r]\{\tau\} \tag{25}$$

where $[I_0^r]$ is a matrix of influence coefficients for the vertical displacements of points along the surface. The displacements are evaluated at N_f points along the surface. Hence, vector $\{\rho_0^r\}$ is of size N_f and vector (s) is of size N while matrix is of size $N_f \times N$ and $I_{0kj}^r = I_{0kj}^{r1} + I_{0kj}^{r2}$

Equation 25 is rewritten as

$$\{\rho_0^r\} = \frac{B_f}{G_s}\{I_0\}q \tag{26}$$

where $\{I_0\}$ is a vector of the Settlement Reduction Coefficients (SRC), defined as

$$SRC_k = I_{0k} = \frac{\rho_{0k}^r G_s}{B_f q} \tag{27}$$

Vector $\{I_0\}$ is obtained as

$$\{I_0\} = [I_0^r]\{\tau\} \tag{28}$$

Results

For the purpose of integration, the loaded area is divided into elements of size $0.025B_f \times 0.025B_f$. The size of the elements along the strip is $0.1B_f \times 0.1B_f$. The influence coefficient, for the vertical displacement of node i, due to normal stress on element j, is evaluated by dividing the element j into 20×20 sub-areas for $abs(i-j) \leq 2$. Coarser subdivision into 4×4 sub-areas was found to be adequate for sub-areas with $abs(i-j) > 2$. The half-width of the strips $B_f = 0.05\ B_f$.

A parametric study brings out the effects of depth, U_0/B_f, length ratio, L_r/B_r, the elongation ratio K_τ of the strip reinforcement and the aspect ratio of the loaded area, L_r/B_r on the mobilised shear stresses, τ, the Settlement Reduction Coefficient (SRC) along the surface and the SRC at the centre of the loaded area, I_{sc}. All results are for a Poisson's ratio $\nu_s = 0.3$.

To check the accuracy of the numerical integration, SRCs obtained at the centre of the loaded area for uniform stresses at depth are compared with those from the exact solution given by Vaziri et al. (1982), (Table 1) and found to agree closely.

Figure 5 shows the variation of the normalised shear stresses, τ/q, with distaricc, x/B_f, along the half-length of an inextensible strip of length, $L_r/B_f = 2$, for various depths, U_0/B_f, below a square loaded area ($L_r/B_f = 1$). The stresses in this figure and all other figures depicting stresses are the total stresses mobilised at the soil-strip interface. These stresses may be assumed to be acting in equal proportion over the top and bottom surfaces of the strip. Due to symmetry, stresses along half the length of the strip are only considered. A positive shear stress is one that prevents outward lateral movement and as such is directed inwards.

Table 1: Comparison of Computed Values of I_{sc} with Exact Solution for Uniform Stresses ($L_r/B_f = 1$).

U_0/B_f	Exact Solution (Vaziri et.al., 1982)	Computed Values
0.25	0.0115016	0.011520
0.50	0.0113095	0.011315
1.00	0.0068968	0.006898
1.50	0.0041129	0.004113
2.00	0.0026271	0.002627

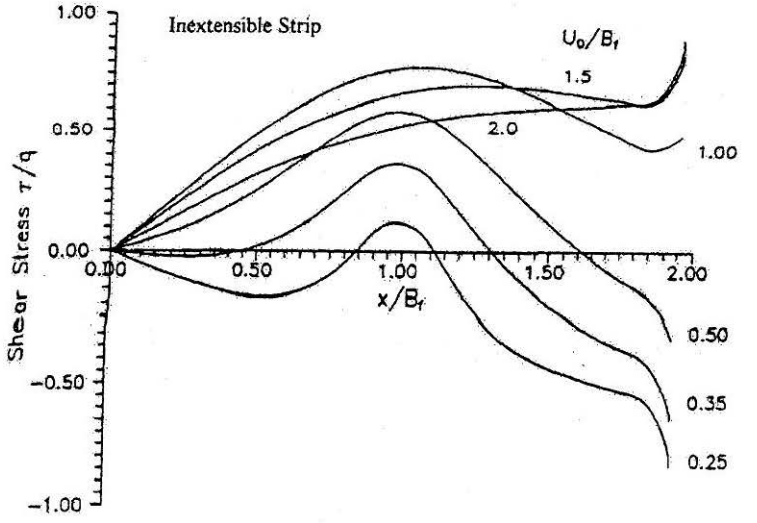

FIGURE 5 : Variation of Shear Stresses with Distance – Effect of Depth of Placement of Strip ($L_r/B_f = 2$; $L_f/B_f = 1$)

In the figure, as intuitively felt, the shear stress at the centre, i.e. at $x/B_f = 0$ is zero. For strips at shallower depths, i.e. $U_0/B_f = 0.25$, the shear stresses are negative over a large portion of the strip. Positive shear stresses are mobilised only for x/B_f in the range 0.85 to 1.1. With increasing depths of placement, the shear stresses are positive over most of the length of the strip. The sharp increase in shear stresses observed at the extreme end of the strip is because the strip is assumed to be inextensible. For depths of placement U_0/B_f upto 1.0 the shear stresses increase up to a distance, $x/B_f = 1$ along the strip and decrease gradually beyond. The increase in stresses is attributed to increasing displacements over the distance, $x/B_f = 0$ to 1. Larger the displacement, higher is the shear stress mobilised. Beyond $x/B_f = 1$, the displacements reduce for $U_0/B_f \leq 1.0$ and hence the stresses mobilised are also smaller. For strips placed at depths $U_0/B_f > 1.0$ the stresses are smaller as compared to those for $U_0/B_f = 1.0$ because the displacements are smaller but the stresses become more or less uniform beyond $x/B_f = 1$ along the strip.

The variation of the normalised shear stress, τ/q, with the distance x/B_f along the length of an extensible strip of length, $L_r/B_f = 2$ placed below a square loaded area at a depth of $U_0/B_f = 1.0$ for various values of K_τ is depicted in Fig. 6. For a highly extensible strip with $K_\tau = 5$, the stresses mobilised are the least, with the edge of the strip showing negative stresses. With an increase in the K_τ value, the stresses increase and are positive throughout the length. For strips with $K_\tau = 5000$, the shear stresses

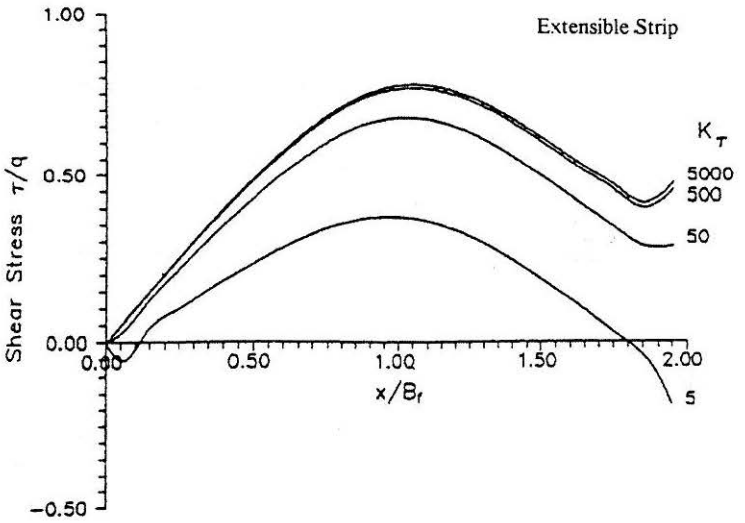

FIGURE 6 : Variation of Shear Stresses with Distance – Effect of Elongation Ratio of Strip ($L_r/B_f = 2$; $L_f/B_f = 1$; $U_0/B_f = 1$)

are the same as those for an inextensible strip (Fig. 5). The maximum shear stress $\tau/q = 0.8$ in this case and is observed at a distance, $x/B_f = 1.0$. The net lateral displacements for an extensible strip are high owing to the high elongations experienced by the strip. Hence, the displacements, which the shear stresses have to counteract, are less, resulting in low shear stress values. As K_τ increases, the elongations in the strip decrease, consequently the displacements to be resisted by the mobilised shear stresses increase significantly. As a result inextensible strips show high shear stresses as compared to extensible ones.

The effect of the length of the inextensible strip on the shear stresses is depicted in Fig. 7 for $U_0/B_f = 1.0$ and $L_r/B_f = 1$. For shorter strips $L_r/B_f = 1$, the shear stresses increase almost linearly over the length of the strip. For strips with $L_r/B_f > 1$, it is interesting to note that the stresses increase to a value of 0.8q at a distance, $x/B_f = 1$, i.e. beneath the edge of the loaded area and then decrease monotonically. For strips of length $L_r/B_f = 2$, the stresses are positive over the whole length of the strip. For strips longer than $2.5B_f$ the mobilised shear stresses become negative over a distance, $x/B_f > 2.5$. It is worthwhile to note that for any length of the strip ($L_r > B_f$), the stresses are positive up to a maximum distance of $2.5B_f$ and are independent of the ratio L_r/B_f. At distance, $x/B_f > 2.5$ and depth $U_0/B_f = 1.0$, the soil displacements due to the surface loading are inward, i.e. towards the centre. As a result the stresses mobilised are negative.

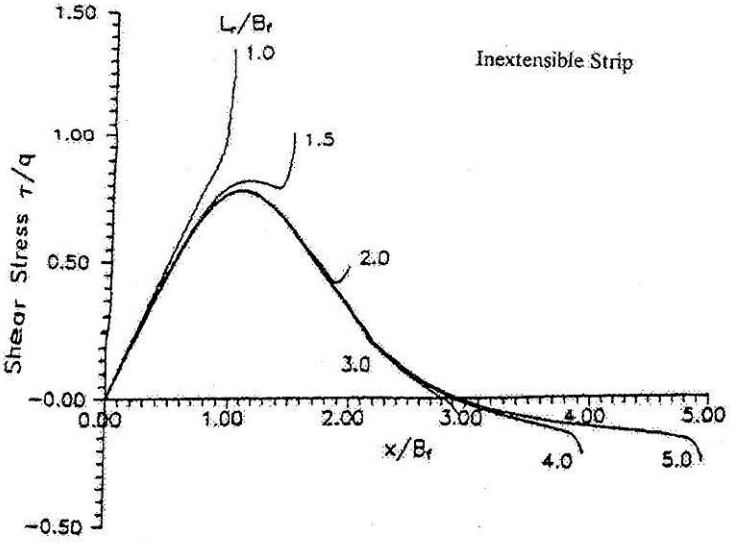

FIGURE 7 : Variation of Shear Stresses with Distance – Effect of Length of Strip ($U_0/B_f = 1$; $L_f/B_f = 1$)

The effect of the shape of the applied load, as defined by the aspect ratio, $L_r > B_f$, on the shear stress distribution is presented in Fig. 8 for an inextensible strip of length $L_r/B_f = 2$ and placed at a depth $U_0/B_f = 1.0$. The stresses are a maximum for a rectangular area with $L_r/B_f = 2$ and a maximum, τ/q of 1.0 is observed at a distance $x/B_f = 1$. Stresses mobilised for areas with $L_r/B_f = 5$ are slightly smaller than those for a rectangle with $L_r/B_f = 2$ but are higher as compared to stresses for a square area or a strip with $L_r/B_f = 10$. As the aspect ratio increases beyond 2, the horizontal displacements start decreasing beyond a depth $U_0/B_f = 1.0$. This results in reduced stress mobilisation.

The variation of normalised tension, $T/q B_f^2$, induced in an extensible strip of length, $L_r/B_f = 2$ placed below a square area at a depth $U_0/B_f = 1.0$, for various K_τ values is presented in Fig. 9. The tension for the strip, with $K_\tau = 5$ is the least owing to low shear stress mobilisation. Strips with $K_\tau = 5000$, exhibit a normalised tension of 0.105, equivalent to that of an inextensible strip. For highly extensible strips with $K_\tau = 5$, the tension at the centre is 0.038.

Figure 10 depicts the effect of K_τ on the elongation, $\rho E_s/B_f q$, of the extensible strip of length, $L_r/B_f = 2$ placed below a square area at a depth $U_0/B_f = 1.0$. As expected, highly extensible strips with $K_\tau = 5$ show maximum extension. The total normalised elongation of these strips is of the order of 0.067. The elongation is maximum at a distance, $x/B_f = 1.5$ along

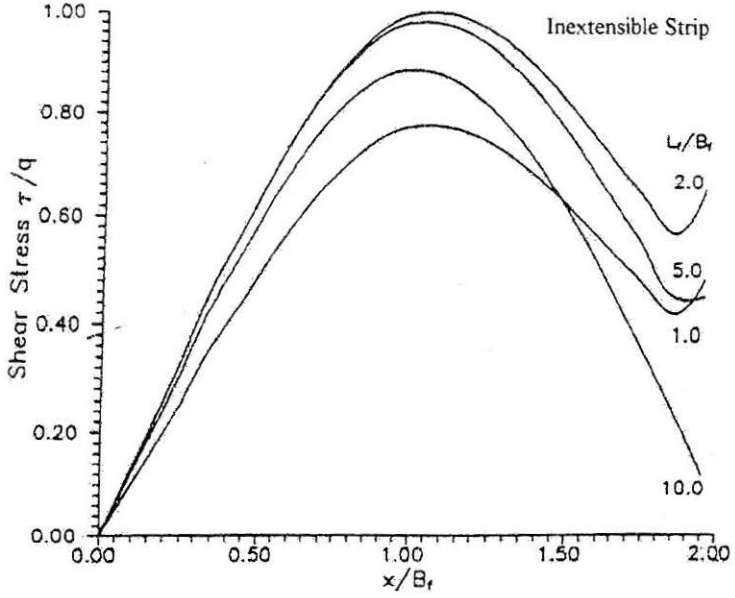

FIGURE 8 : Variation of Shear Stresses with Distance – Effect of Aspect Ratio of Loaded Area ($L_r/B_f = 2$; $U_0/B_f = 1$)

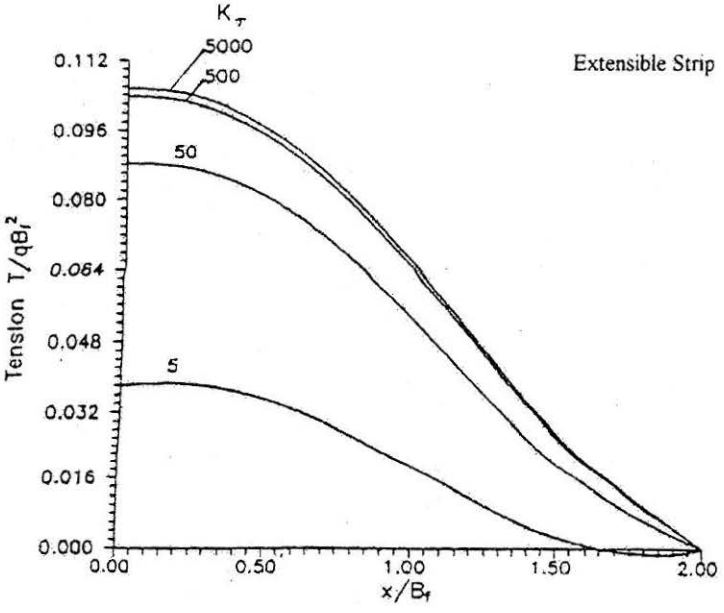

FIGURE 9 : Variation of Tension with Distance – Effect of Elongation Ratio of Strip ($L_r/B_f = 2$; $L_f/B_f = 1$; $U_0/B_f = 1$)

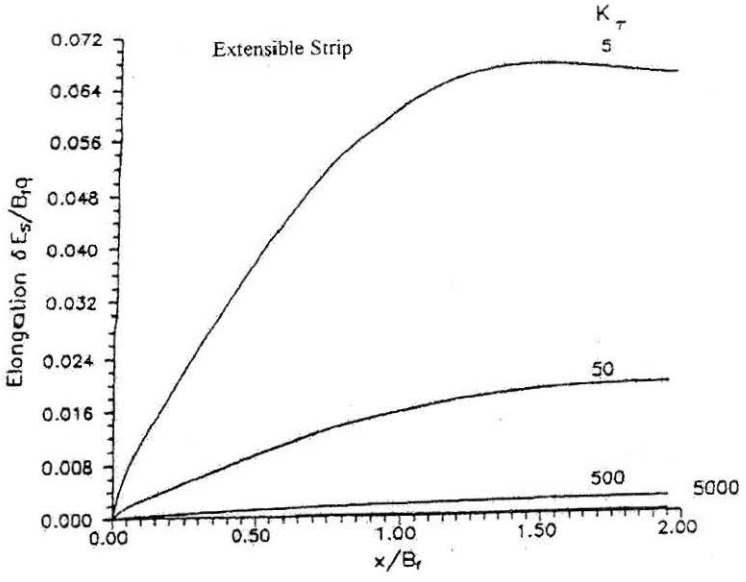

FIGURE 10 : Variation of Elongation with Distance – Effect of Elongation Ratio of Strip ($L_r/B_f = 2$; $L_f/B_f = 1$; $U_0/B_f = 1$)

the length of the strip. Beyond this distance, it decreases marginally as the strip is subjected to a small amount of compression in this zone. Elongation of the strips decreases with increase in K_τ, as anticipated.

Figure 11 depicts the variation of SRC with distance, x_f/B_f, along the half-width of the loaded area for different lengths, L_r/B_f of an inextensible strip placed below a square area at a depth, $U_0/B_f = 1.0$. A positive SRC indicates heave while a negative one indicates settlement of the surface. For all lengths of the strip, the SRC values are maximum at the centre of the loaded area ($x_f/B_f = 0$) and gradually decreases with increase in the distance. It is also noted that SRC values increase with increasing length of the reinforcement strip. The improvement in SRC for the length L_r/B_f increasing from 1 to 2 is significant while it is not very significant when L_r/B_f increases from 2 to 5. The SRC at the centre for L_r/B_f = 2 and 5 are 0.00335 and 0.0035 respectively. Thus, at a depth, $U_0/B_f = 1.0$, no advantage accrues by providing reinforcements of lengths greater than twice the width of the loaded area when shear interaction alone is considered. A strip of length equal to B_f gives an SRC of 0.0023 at the origin and a small negative value at the edge. The increase in SRC for L_r/B_f increasing from 2 to 5 is marginal because as the strip length increases shear stresses are negative beyond a distance x/B_f = 2.5 as is depicted in Fig.7 and are responsible for settlement of the surface.

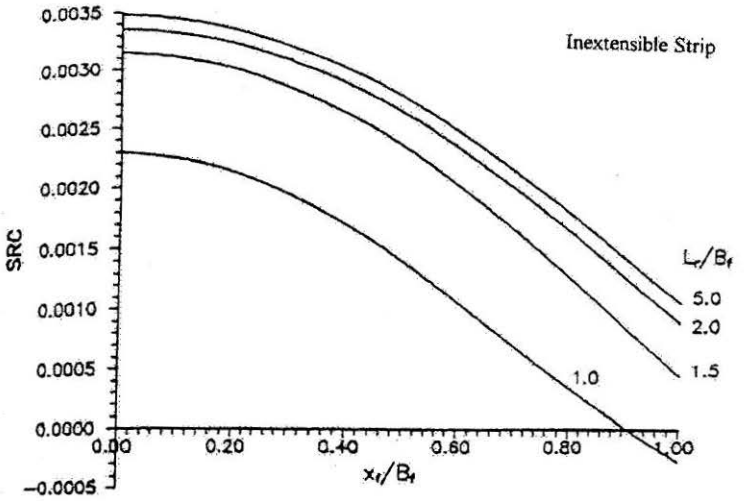

FIGURE 11 : Variation of SRC with Distance along Surface – Effect of Length of Strip ($U_0/B_f = 1$; $L_f/B_f = 1$)

The effect of depth, U_0/B_f, on the SRC for an inextensible strip of length, $L_r/B_f = 2$, placed below a square area is presented in Fig. 12. It is seen that except for $U_0/B_f = 0.25$, for all other depths, the SRC is maximum at the centre of the loaded area and decreases with distance, x_f/B_f. It is interesting to note that for a depth of $U_0/B_f = 0.25$, the maximum SRC is observed at a distance $x_f/B_f = 0.75$. This is because, for this depth the stresses are predominantly negative. With increasing depths, the SRC is positive and the rate of change of SRC with x_f/B_f decreases. The maximum SRC is observed for $U_0/B_f = 1.0$ beyond which the SRC decreases because the stresses beyond this depth also decrease.

The variation of SRC for different aspect ratios, L_r/B_f, of the loaded area for inextensible strips of length, $L_r/B_f = 2$, placed at a depth, $U_0/B_f = 1.0$ is depicted in Fig. 13. The maximum SRC is observed for a rectangular area with $L_r/B_f = 2$. The increase in SRC for L_r/B_f increasing from 1 to 2 is appreciable. For larger rectangles the SRC are smaller.

The variation of SRC for different elongation ratios, K_τ for an extensible strip of length, $L_r/B_f = 2$ placed below a square area at a depth, $U_0/B_f = 1.0$ is shown in Fig. 14. The SRC is low for highly extensible strips ($K_\tau = 5$) because the stresses mobilised at the interface are small. As K_τ increases SRC increase and coincide with those for an inextensible strip with centre and edge showing SRC values of 0.00335 and 0.0009 respectively.

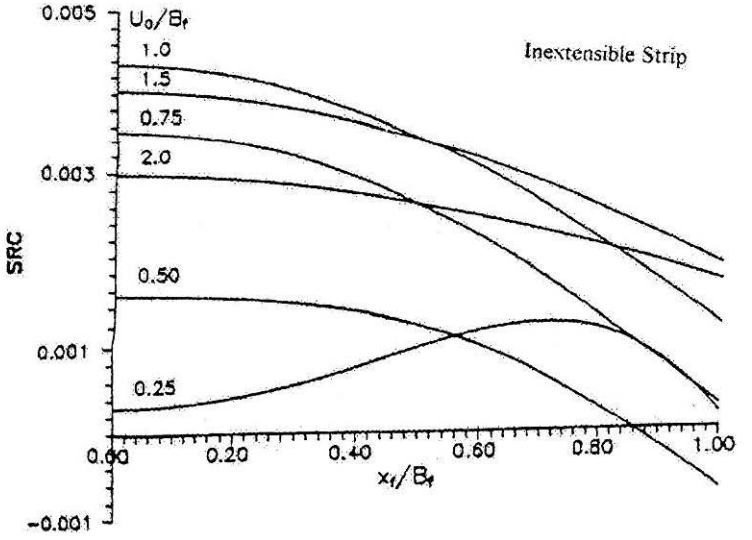

FIGURE 12 : Variation of SRC with Distance along Surface – Effect of Depth of Placement of Strip ($L_r/B_f = 2$; $L_f/B_f = 1$)

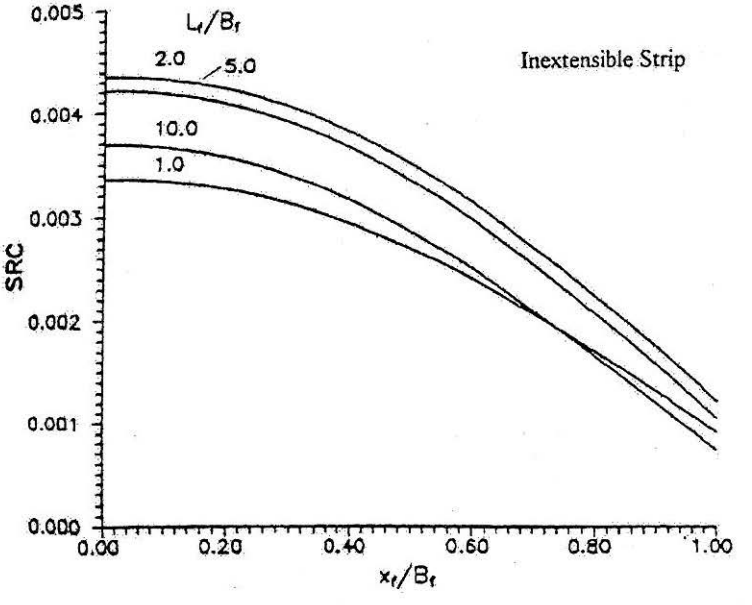

FIGURE 13 : Variation of SRC with Distance along Surface – Effect of Aspect Ratio of Loaded Area ($L_r/B_f = 2$; $U_0/B_f = 1$)

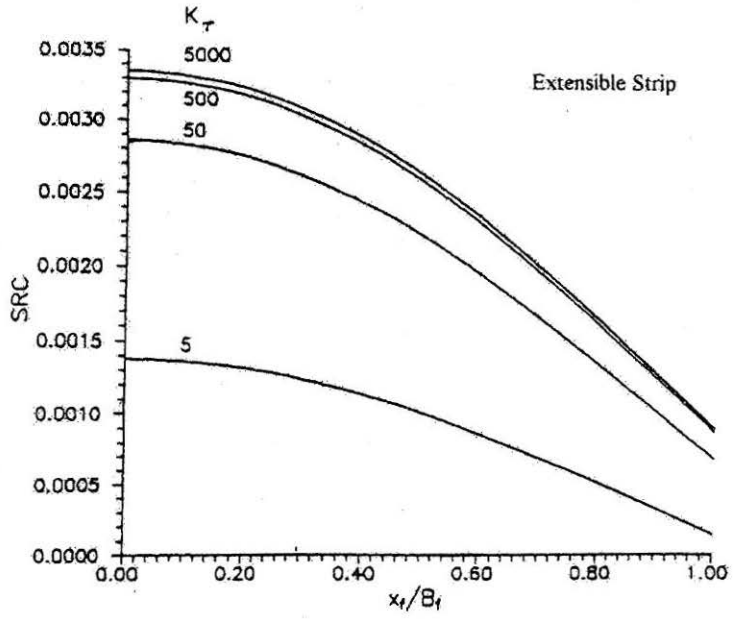

FIGURE 14 : Variation of SRC with Distance aling Surface – Effect of Elongation Ratio of Strip ($L_r/B_f = 2$; $L_f/B_f = 1$; $U_0/B_f = 1$)

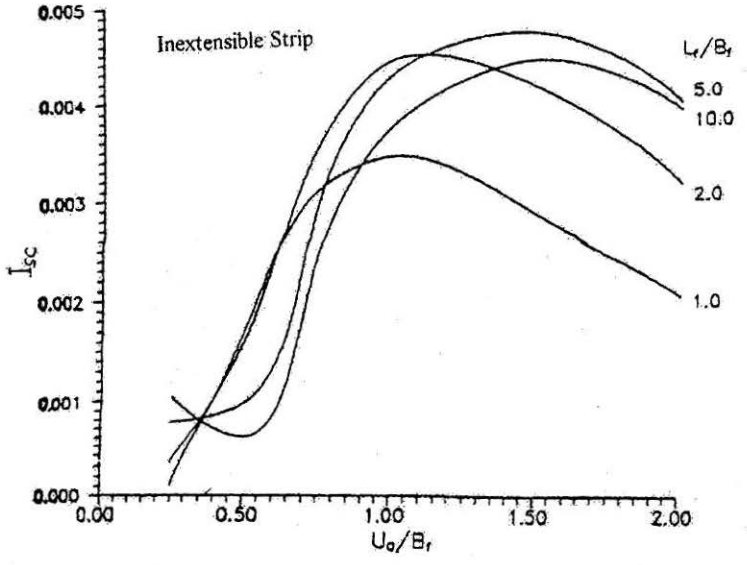

FIGURE 15 : Effect of Depth of Placement of Strip and Aspect Ratio of Loaded Area on I_{sc} ($L_r/B_f = 2$)

The effect of U_0/B_f on the settlement reduction coefficient at the centre of the loaded area, I_{sc}, for different aspect ratios of the loaded area for an inextensible strip of length, $L_r/B_f = 2$ is presented in Fig. 15. It is observed that for square and rectangular areas with $L_f/B_f = 2$, I_{sc} increase with depth and reaches maximum values at around $1.0B_f$. The values respectively are 0.0034 and 0.0044. In the case of longer areas the maximum I_{sc} is observed at greater depths. The maximum I_{sc} for $L_f/B_f = 5$ almost matches with that for $L_f/B_f = 2$ but is lower for $L_f/B_f = 10$.

Figure 16 presents the effect of K_τ on I_{sc} for different depths, U_0/B_f of an extensible strip of length $L_f/B_f = 2$ placed below a square area. I_{sc} is a maximum in the depth range, $U_0/B_f = 0.75$ to 1.0 depending on the values of K_τ. For highly extensible strips ($K_\tau = 5$) a maximum I_{sc} value of 0.0015 is observed at a depth $U_0/B_f = 0.75$. At very shallow depths, $U_0/B_f = 0.25$, the I_{sc} values are practically zero. As K_τ increases, the I_{sc} values at all depths tend to those of an inextensible strip. The maximum I_{sc} value for a strip with $K_\tau = 5$ is around 0.45 times that for an inextensible strip.

Conclusions

An analysis using the elastic continuum approach for studying the shear interaction along a single embedded strip below a uniformly loaded

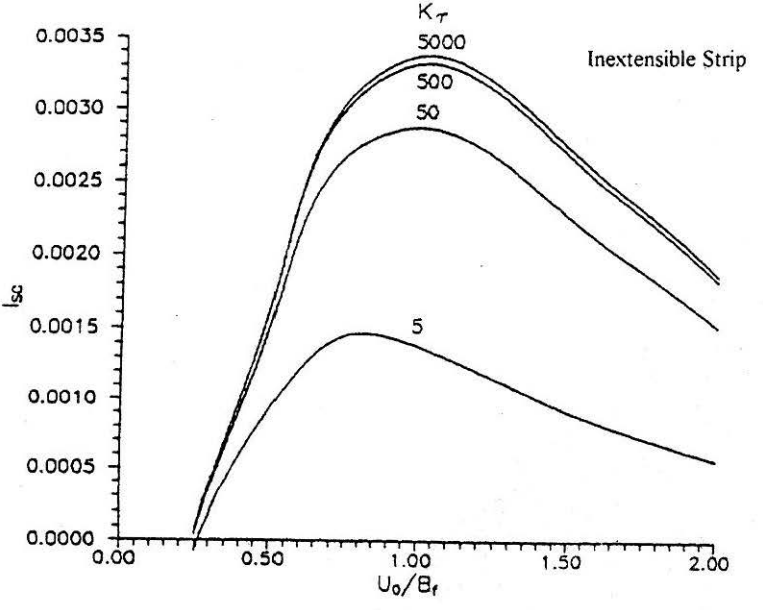

FIGURE 16 : Effect of Depth of Placement and Elongation Ratio of Strip on I_{sc} ($L_r/B_f = 2$; $L_f/B_f = 1$)

rectangular area is proposed. The analysis is based on the concept that the lateral displacements produced by the surface load are opposed by mobilised shear stresses at the soil-reinforcement interface. The extent of lateral deformations opposed would depend on the axial stiffness of the reinforcing strip and this would reflect on the magnitude of the shear stresses mobilised at the interface. In order to evaluate the shear stresses, the compatibility of horizontal displacements at points along the soil-strip interface and the equilibrium of forces are satisfied. In satisfying the displacement compatibility an inextensible strip as well as an extensible one are considered. An elongation ratio K_r is defined for an extensible strip. The tension developed in inextensible and extensible strips due to the mobilised shear stresses is evaluated. The elongations of the extensible strip are also computed. The reduction in surface settlements due to the mobilised shear stresses is evaluated.

A parametric study was carried out to study the effect of the aspect ratio of the loaded area, length and depth of placement of the reinforcing strip and axial stiffness of the strip on the shear stresses developed at the interface and on the reduction of surface settlements.

It is concluded from the analysis that, for shear interaction alone, strips placed at shallow depths ($U_0/B_f < 0.75$) are ineffective. The optimum location would be 0.75 to $1.0B_f$ below rectangular areas with aspect ratio of up to 2. As the aspect ratio of the loaded area increases the optimum depth of placement increases and is around $1.5B_f$ for strip type of loading. Strips of length 2 to 2.5 times the width of the loaded area contribute to the maximum settlement reduction. No additional benefit is gained by providing longer strips. In comparison to the settlement reduction acheived from normal stress interaction (Pitchumani and Madhav, 1994), shear stresses contribute to a smaller extent. Performance of extensible strips approach that of inextensible ones with increase in the elongation ratio which depends on the relative stiffnesses of the strip and soil.

References

ANDRAWES, K.Z. and McGOWN, A. (1982) : "Finite Element Method of Analysis Applied to Soil-Geotextile System", *Proc. II Intl Conf. on Geotextiles*, Las Vegas, *Vol.3, pp.695-699.*

BINQUET, J. and LEE, K.L. (1975) : "Bearing Capacity Analysis of Reinforced Earth Slabs", *Jl. of Geotech. Engrg. Div.*, ASCE, Vol.101, No.GT12, pp.1257-1276.

DEMBICKI, E. and ALENOWICZ, J.M. (1988) : "Influence of Geotextile on Bearing Capacity of Two Layered Subsoils", *Proc. Ist Indian Geotextiles Conf.*, Bombay, Vol.1, pp.A61-A66.

FRAGASZY, J.P. and LAWTON, E. (1984) : "Bearing Capacity of Reinforced Sand Subgrades", *Jl. of Geotech. Eng. Div.*, ASCE, Vol.110, No.GT10, pp.1500-1507.

GIROUD, J.P. and NOIRAY, L. (1981) : "Geotextile-reinforced Unpaved Road Design", *Jl. of Geotech. Eng. Div.*, ASCE, Vol.107, No.GT9, pp.1233-1254.

HOULSBY, G.T. and JEWELL, R. (1990) : "Design of Reinforced Unpaved Roads for Small Rut Depths", *Proc. IV Int. Conf on Geotextiles and Geomembranes*, The Hague, Vol.1, pp.171-176.

HUANG, C.C. and TATSUOKA, F. (1988) : "Prediction of Bearing Capacity on Level Sandy Ground reinforced with Strip Reinforcement", *Proc. Int. Geotechnical Symp. on Theory and Practice of Earth Reinforcement*, Fukuoka, pp.191-196.

JONES, R.H. and DAWSON, A.R. (1990) : "Reinforced Soil Foundations for Buildings", *Proc. Intl. Reinforced Soil Conf.*, Glasgow, pp.477-478.

LOVE, J.P., BURD, H.J., MILLIGAN, G.W.E. and HOULSBY, G.T. (1990) : "Analytical and Model Studies on Reinforcement of a Layer of Granular Fill on Soft Clay Subgrades", *Canadian Geotech. Jl.*, Vol.24, pp.611-622.

MADHAV, M.R. and GHOSH, C. (1988) : "Modelling for Settlement Analysis of Reinforced Soils", *Proc. 1st Indian Geotextiles Conf.*, Bombay, Vol.1, pp.C33-C40.

MADHAV, M.R. and PITCHUMANI, N.K. (1992) : "Settlement Reduction due to Reinforcement Strip", *Proc. Intl. Sym. on Earth Reinforcement Practice*, Fukuoka, pp.631-636.

MADHAV, M.R. and PITCHUMANI, N.K. (1996) : "Numerical Modelling and Analysis of Reinforcement Strip-Soil Interactions", *Proc. 2nd Intl. Conf. in Civil Engg. on Computer Applications, Research and Practice*, Bahrain, pp.579-586.

MIURA, N., SAKAI, A., TAESIRI, Y., MOURI, K. and OHTSUBO, M. (1988) : "Model and Field Tests of Reinforced Pavement on Soft Clay Ground", *Proc. Int. Geotechnical Symp. on Theory and Practice of Earth Reinforcement*, Fukuoka, pp.227-232.

PITCHUMANI, N.K. (1992) : "Reinforced Foundation Beds : Soil-Reinforcement Interaction Analyses", *Doctoral Thesis*, IIT Kanpur, p.278.

PITCHUMANI, N.K. and MADHAV, M.R. (1994) : "Soil-Reinforcement Strip Interaction Analysis", *Computer Methods and Advances in Geomechanics*, eds. Siriwardane & Zaman, Balkema, pp.1403-1408.

PITCHUMANI, N.K. and MADHAV, M.R. (1997) : "Analysis of Flexible Reinforcement Strip-Soil Interaction", *Computer Methods and Advances in Geomechanics*, ed. Yuan, Balkema, pp.2349-2354.

POULOS, H.G. and DAVIS, E.H. (1975) : *Elastic Solutions for Soil and Rock Mechanics*, Wiley Intl, New York.

SRIDHARAN, A., MURTHY, B.R.S., BINDUMADHAVA, and VASUDEVAN, A.K. (1988) : "Reinforced Soil Foundation on Soft Soil", *Proc. 1st Indian Geotextiles Conf.*, Bombay, Vol.1, pp.C53-C60.

VAZIRI, H., SIMPSON, B., PAPPIN, J.W. and SIMPSON, L. (1982) : "Integrated Form of Mindlin's Equations", *Geotechnique*, Vol.32, pp.275-278.

Notations

B_f = Half-width of loaded area

B_r = Half-width of reinforcement strip

c = Depth at which force acts (Mindlin's Problem)

dA = elemental area

E_s = Modulus of deformation of soil

G_s = Shear modulus of soil

I_{sc} = Settlement Reduction Coefficient at center of loaded area

K_τ = Elongation Ratio for extensible strip

L_f = Half-length of loaded area

L_r = Half-length of strip reinforcement

n_B = Number of sub-elements along width of loaded area

n_L = Number of sub-elements along length of loaded area

N = Number of elements along half-length of strip

q = Intensity of loading on surface

SRC = Settlement Reduction Coefficient

U_0 = Depth of placement of strip

x, y, z = Cartesian co-ordinates

ν_s = Poisson's ratio of soil

ρ_{xi} = Horizontal displacement of point i

τ = *Shear stress mobilised at soil-strip interface.*